Metal Ion Coordination in Copper and Nickel Reconstituted Hemoglobins

Periakaruppan T. Manoharan,*† Kenneth Alston,‡ and Joseph M. Rifkind†

Contribution from the Laboratory of Cellular and Molecular Biology, Gerontology Research Center, NIH/NIA, Baltimore, Maryland 21224, and the Department of Natural Sciences, Benedict College, Columbia, South Carolina 29204. *Received November 5, 1985*

Abstract: The origin of the complex visible spectra of Ni(II)- and Cu(II)-substituted human hemoglobin A (NiHbA and CuHbA) was studied. The visible spectra of these hemoglobins were compared with those for metal-substituted isolated subunits and myoglobin. Also, electron paramagnetic resonance spectral studies were performed on the paramagnetic Cu(II) proteins. It was shown that two distinct metal ion environments exist in these proteins: I, a five-coordinated complex with a strong proximal histidine bond with significant σ- and π-bonding, and II, a complex with much weaker axial ligation. The five-coordinated complex is detected for myoglobin, while the type II complex with weaker axial ligation is found for isolated α-chains. Subunit interactions in both hemoglobin A as well as hemoglobin H (the tetramer consisting of four β-subunits) produce a mixture of both types of coordination.

One of the most interesting problems in heme proteins is the relationship between protein conformation and function.[1] The functional role centers on the heme iron which is recognized as the principal site of interaction with the substituent ligands and inhibitors. This important role of the porphyrin metal on the function has been emphasized in the crystallographic studies of metalloporphyrins and hemoglobins.[1-3] It is in this context that the substitution of the natural iron porphyrin moiety of hemoglobin with other transition-metal porphyrins has proved to be an important tool in the investigation of the intrinsic role of the central metal ion.[4,5] Earlier work on metal reconstituted hemoglobins has primarily focused on cobalt[4-18] as the central ion. From these studies it was possible to elucidate the structure of the metal–dioxygen bond,[5,6] to refine the triggering mechanism for the allosteric transition,[4-6] to understand the role of the metal in determining the protein conformation,[17] and to evaluate the influence of globin on the thermodynamics of ligand binding.[18]

Some of the recent work[19-24] on nickel and copper reconstituted hemoglobins reveal certain interesting features which differ from those of cobalt and iron. Thus, reconstituted hemoglobins with nickel(II) and copper(II) at the porphyrin site do not bind oxygen in contrast to the reversible oxygen-binding property of iron and cobalt hemoglobins. Immunochemical studies have shown[23] that the substitution of nickel for iron in hemoglobin (NiHbA) yields a molecule that is antigenically distinct from R-state oxy-, carboxy-, and methemoglobin A. This protein is said to be in the T state based on further evidence from X-ray crystallography, circular dichroism (CD), and sulfhydryl reactivity.[19] Sulfhydryl reactivity studies on CuHb also confirm that CuHb has a T-like protein conformation similar to that of NiHb.[24]

The optical spectra of NiHbA and CuHbA indicate an unusual split Soret band. In an attempt to explain the origin of this visible spectrum, studies have been performed on myoglobin and isolated subunits.

Electron spin resonance (ESR), which is a particularly powerful method for probing coordination of paramagnetic metal ions, was used to help define the type of coordination found in the Cu(II)-substituted hemoglobins. It was thus possible to demonstrate the presence of two distinct metal ion geometries in CuHbA. A comparison of the visible spectra of NiHbA with that of CuHbA suggests that NiHbA also possesses two distinct metal ion geometries similar to those found in CuHbA.

The existence of two types of active sites in R-state oxy-CoHbA has been identified by Yonetani and co-workers[13,16] from EPR spectral information. These studies on T-state NiHbA and CuHbA provide new information relating the metal ion environment to subunit interactions.

Table I. Absorption Band Maxima of Nickel- and Copper-Substituted Heme Proteins

protein	Soret, nm		visible, nm		
Ni^{II}HbA	399	418	517	556	579
Ni^{II}-α-SH	399		520	556	
Ni^{II}-β-SH	399	418	517	556	579
Ni^{II}Mb		424		541	584
Cu^{II}HbA	405	418	536	569	
Cu^{II}Mb		425		545	585

* On leave from the Department of Chemistry, Indian Institute of Technology, Madras 600 036, India.
† Gerontology Research Center.
‡ Benedict College.

(1) Antonini, E.; Brunori, M. *Hemoglobins and Myoglobins in Their Rections with Ligands*; North Holland: Amsterdam, 1971
(2) Perutz, M. F. *Nature (London)* **1970**, *228*, 726.
(3) Hoard, J. L. In *Hemes and Heme Proteins*; Chance, B., Estabrook, R. W., Yonetani, T. Eds.; Academic: New York, 1971; pp 9–24.
(4) Hoffman, B. M.; Petering, D. H. *Proc. Natl. Acad. Sci. U.S.A.* **1970**, *67*, 637.
(5) Chien, J. C. W.; Dickinson, L. C. *Proc. Natl. Acad. Sci. U.S.A.* **1972**, *69*, 2783.
(6) Dickinson, L. C.; Chien, J. C. W. *J. Biol. Chem.* **1973**, *248*, 5005; *Biochem. Biophys. Res. Commun.* **1973**, *51*, 587.
(7) Hoffman, B. M.; Gibson, Q.-H.; Bull, C.; Crepean, R. H.; Edelstein, S. J.; Fisher, R. G.; McDonold, J. *Ann. N. Y. Acad. Sci.* **1975**, *244*, 174.
(8) Yonetani, T.; Yamamoto, H.; Iizuka, T. *J. Biol. Chem.* **1974**, *249*, 2168.
(9) Hsu, G. C.; Spilburg, C. A.; Bull, C.; Hoffman, B. M. *Proc. Natl. Acad. Sci. U.S.A.* **1972**, *69*, 2122. Hoffman, B. M. In *Porphyrins*; Dolphin, D., Ed.; Academic: New York, 1979; Part B, pp 403–444.
(10) Srivastava, T. S.; Yonetani, T. *Proc. Fed. Am. Soc. Exp. Biol.* **1974**, *33*, 1449.
(11) Yonetani, T.; Yamamoto, H.; Woodrow, G. V., III *J. Biol. Chem.* **1974**, *249*, 682.
(12) Yamamoto, H.; Kayne, F. J.; Yonetani, T. *J. Biol. Chem.* **1974**, *249*, 691.
(13) Ikeda-Saito, M.; Yamamoto, H.; Imai, K.; Kayne, F. J.; Yonetani, T. *J. Biol. Chem.* **1977**, *252*, 620.
(14) Imai, K.; Yonetani, T.; Ikeda-Saito, M. *J. Mol. Biol.* **1977**, *109*, 83.
(15) Imai, K.; Ikeda-Saito, M.; Yamamoto, H.; Yonetani, T. *J. Mol. Biol.* **1980**, *138*, 635.
(16) Inubushi, T.; Yonetani, T. *Biochemistry* **1983**, *22*, 1894.
(17) Chien, J. C. W.; Synder, F. W., Jr. *J. Biol. Chem.* **1976**, *251*, 1670.
(18) Spilburg, C. A.; Hoffman, B. M.; Petering, D. H. *J. Biol. Chem.* **1972**, *247*, 4219.
(19) Alston, K.; Schechter, A. N.; Arcoleo, J. P.; Greer, J.; Parr, G. R.; Friedman, F. K. *Hemoglobin* **1984**, *8*, 47.
(20) Alston, K.; Friedman, F. K.; Schechter, A. N. *Hemoglobin* **1982**, *6*, 15.
(21) Alston, K.; Park, C. M.; Rodgers, D. W.; Edelstein, S. J.; Nagel, R. L. *Blood*, in press.
(22) Manoharan, P. T.; Alston, K.; Rifkind, J. M. *Bull. Mag. Res.* **1983**, *5*, 255.
(23) Alston, K.; Dean, A.; Schechter, A. N. *Mol. Immunol.* **1980**, *17*, 1475.

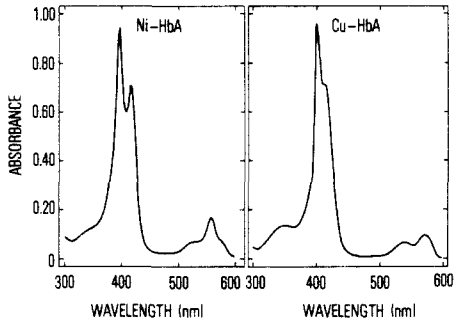

Figure 1. Visible spectra of NiHbA and CuHbA in 0.05 M phosphate, pH 7.4, at room temperature.

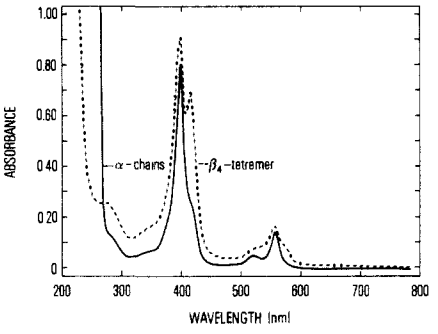

Figure 2. Visible spectra of Ni^{II}-α-SH and Ni^{II}-β-SH in 0.05 M phosphate, pH 7.4, at room temperature.

Experimental Section

CuHbA and NiHbA were prepared according to the methods reported earlier.[19] In preparing ^{63}CuHbA, ^{63}CuO (99.89% pure) purchased from Union Carbide Corp., Oak Ridge National Laboratories, was used after converting it into the acetate form. CuMb and NiMb were prepared by the method of Alston and Storm.[25]

ESR spectra were measured in the temperature region 10–300 K by using a JEOL-JES-ME-1 X-band ESR instrument. The temperature was regulated by an Air Products cryogenic unit with an Air Products temperature controller. Q-band frequency measurements were made by using a Varian E-112 ESR instrument equipped with a similar low-temperature unit. All measurements were made at 100-kHz field modulation and with DPPH as the g marker. The magnetic field sweep was calibrated using Mn^{2+} in SrO. Optical spectra were recorded on a Varian-Cary 219 spectrophotometer.

Computer simulations of the ESR spectra were performed by using a program written for the IBM 370/155 by Dr. Dinesh Nettar, which was modified for the VAX-11 computer.

Results

Visible Spectroscopy. Figure 1 shows the complex visible spectra of NiHbA and CuHbA. For NiHbA, the split soret with peaks at 399 and 418 nm (Table I) and the shoulders on the 556-nm peak at 517 and 579 nm suggest the existence of two spectral components. For CuHbA, the prominent shoulder on the 405-nm Soret band at 418 nm again suggests two spectral components.

Figure 2 shows the visible spectra of the Ni(II) reconstituted chains. For Ni^{II}-α-SH, which consists of monomeric chains, the split Soret is replaced by a single short wavelength peak at 399 nm and a small shoulder in the longer wavelength region of the spectrum. In the visible, two bands are resolved at 520 and 556 nm. This spectrum appears to be dominated by one of the spectral components observed for Ni^{II}HbA. On the other hand, for the Ni^{II}-β-SH chains, which consists of a tetramer, a spectrum very similar to that of Ni^{II}HbA is observed.

For Ni^{II}Mb and Cu^{II}Mb, the visible spectra (Figure 3) demonstrate the presence of predominantly a single spectral component with the Soret bands located at 424 and 425 nm, respectively.

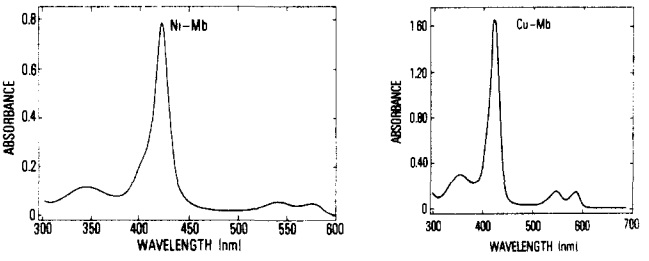

Figure 3. Visible spectra of NiMb and CuMb in 0.05 M phosphate, pH 7.4, at room temperature.

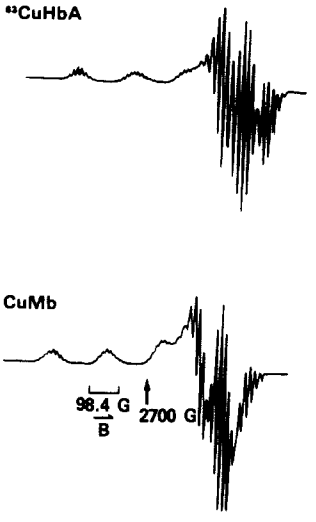

Figure 4. X-band ESR spectra of ^{63}CuHbA and CuMb at 12 K. The spectrum of ^{63}CuHbS is identical with that of CuHbA.

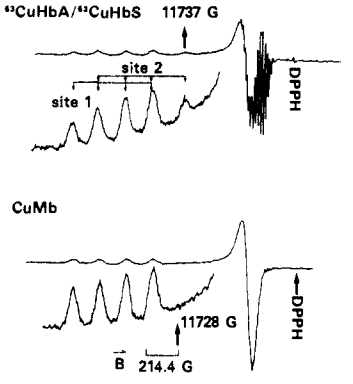

Figure 5. Q-band ESR spectra of ^{63}CuHbA, ^{63}CuHbS, and CuMb at 120 K.

Electron Spin Resonance (ESR). The ESR spectrum of CuHbA with the natural isotropic abundance of ^{63}Cu and ^{65}Cu gave a complex superhyperfine spectra due to ^{14}N on each of the separated parallel components from electron–copper nuclear hyperfine interaction. In order to simplify the spectrum, ^{63}CuHbA was prepared. The spectrum of this protein is compared with that of CuMb in Figure 4 as measured at the X-band frequency. Three points emerge by looking at these spectra. (i) The superhyperfine lines due to ^{14}N are expected to originate from the porphyrin nitrogens and should produce only nine lines on each one of the parallel components due to ^{63}Cu. On the contrary, the X-band CuHbA spectrum reveals the presence of more than nine lines on the parallel components, suggesting the presence of more than one type of copper site. However, the parallel components in CuMb show only the expected nine superhyperfine components on each of the parallel resonances due to ^{63}Cu. (ii) It is clear that $A_{\parallel}$ (^{63}Cu) for CuMb is smaller than that of CuHbA. (iii) Some differences between ^{63}CuHbA and CuMb are apparent in the perpendicular part of the spectra also. It is necessary to point out here that there is no temperature dependence on the ESR

(24) Manoharan, P. T.; Alston, K.; Rifkind, J. M. In *Biochemical and Inorganic Aspects of Copper Coordination Chemistry*; Karlin, K. D.; Zubieta, J., Eds.; Adenine: New York, 1985; pp 105–118.
(25) Alston, K.; Storm, C. B. *Biochemistry* **1979**, *79*, 4292.

Table II. ESR Parameters of Reconstituted Hemoglobins and Myoglobin[a]

reconstituted hemoglobin	$g_\parallel$	$g_\perp$	$A_\parallel(^{63}Cu)$	$A_\perp(^{63}Cu)$	$A_\parallel(^{14}N)$	$A_\perp(^{14}N)$
CuHbA						
site 1	2.217	2.054	179.3	11.7	14.6	14.4
site 2	2.178	2.042	193.6	19.8	14.3	16.5
CuHbS						
site 1	2.215	2.054	177.6	11.7	14.6	14.4
site 2	2.178	2.042	193.6	19.8	14.3	16.5
CuMb[b]	2.214	2.045	178.5	12.0	14.6	14.4

[a] Some of the parameters are different from our earlier results (not based on simulations) presented at the copper conference held at SUNY, Albany, in 1984 (ref 24). Error estimates for $g = \pm 0.001$, for $A = \pm 1.0$. All A values in 10^{-4} cm^{-1}. [b] The values given here for CuMb are slightly different from those given in ref 26 and must be considered correct since the results are derived from simulation of the Q-band spectrum.

spectra except for higher resolution and higher intensity at lower temperature.

The ESR spectra of both of these hemoproteins were also measured at higher frequency (Figure 5) in an attempt to explain the X-band spectra. The ESR spectrum of ^{63}CuHbA clearly indicates the presence of two different copper environments. The parallel lines due to ^{63}Cu completely separate from the perpendicular features at this frequency and contain two sets of four lines partially superimposed. The two sets of lines have almost equal integrated intensities. Again, the perpendicular part of ^{63}CuHbA is made up of two components, one with distinctly narrowed superhyperfine lines and another with broadened unresolved superhyperfine structure. On the other hand, in the spectrum of CuMb the perpendicular part is totally broadened out and has characteristics more similar to one of the sites of ^{63}CuHbA.

Though reasonable ESR parameters can be obtained for the parallel component without recourse to simulations, using the Hamiltonian

$$\mathcal{H} = g_\parallel \beta B_z S_z + g_\perp \beta (B_x S_x + B_y S_y) + A_\parallel S_z I_z + A_\perp (S_x I_x + S_y I_y) + Q'[I_z - 3I(I+1)] + \sum_{\text{lig N}} S A_N I^n \quad (1)$$

computer simulations were needed to obtain the perpendicular components and the relative amounts of species with reasonable accuracy. First the ESR spectrum of CuMb was fitted. By use of the parameters obtained from this fit as a first approximation for site 1 of ^{63}CuHbA, the parameters for site 2 were determined by fitting the Q-band ESR spectra of ^{63}CuHbA by the combined spectra due to sites 1 and 2. The computed Q-band ESR spectra are given in Figure 6a–c, and they could be compared with the experimental spectra shown in Figure 5. In order to have an appreciation of the goodness of the computer fit for ^{63}CuHbA, the sum of the simulated spectra for sites 1 and 2 in the perpendicular region is compared with the experimental spectrum in Figure 6d. The ESR parameters obtained from the X- and Q-band measurements for both reconstituted copper hemoproteins are given in Table II.

Site 1 of CuHbA has g and $A(^{63}Cu)$ tensor values which again are similar to those found for CuMb. Even the hyperfine coupling constants due to ^{14}N nuclei are similar. However, the ESR parameters due to site 2 are quite different from those of site 1 of ^{63}CuHbA and from those of CuMb.

The reliability of the parameters in Table II is indicated by the almost identical values obtained by independently fitting spectra obtained for normal human hemoglobin (^{63}CuHbA) and sickle cell hemoglobin (^{63}CuHbS). HbS has a single amino acid modification near the amino terminus of the β-chain (β-6 Glu → Val), which is not expected to alter the heme environment.

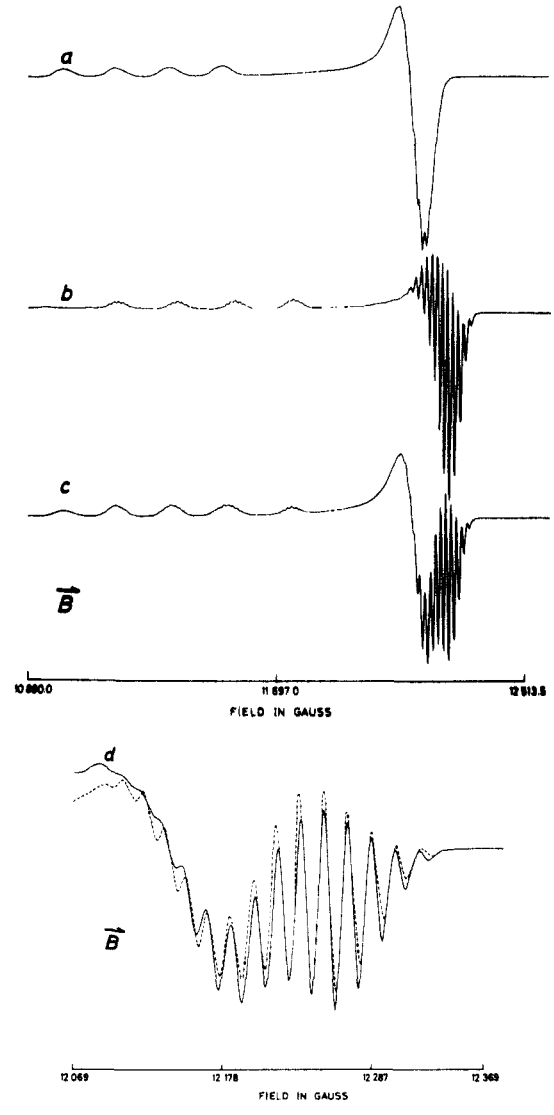

Figure 6. Simulated Q-band ESR spectra of (a) site 1 of ^{63}CuHbA, (b) site 2 of ^{63}CuHbA, (c) combination of sites 1 and 2 in the ratio of 1:1 (cf. Figure 5), and (d) the perpendicular part of the experimental spectrum of ^{63}CuHbA (---) compared with the simulated spectra (—) due to sites 1 and 2 combined in the ration of 1:1. For simulations, ESR parameters given in Table II have been employed. Line width employed for site 1 is 7.5 G and site 2 is 3.5 G.

Discussion

Two Metal Ion Environments in NiHbA and CuHbA. The split Soret band in NiHbA and CuHbA (Figure 1) can be due to either two different metal ion environments or a perturbation which splits the porphyrin $\pi \rightarrow \pi^*$ transition responsible for the Soret band. Similarity of the maxima for the single Soret band in the Ni-α-SH (Figure 2) and Ni–myoglobin (Figure 3) complexes with the short and long wavelength bands (Table I) supports the hypothesis that the metal-substituted hemoglobins have two distinct metal ion environments.

The ESR spectra of ^{63}CuHbA measured at two frequencies (Figures 4 and 5) confirm the presence of two metal ion environments in copper-substituted hemoglobin, with one of them very similar to that found in myoglobin. A delineation of the nature of ligation of the two different porphyrin metal environments can be made from the ESR data of these Cu proteins.

As shown in Table II, all of the ESR spectral parameters for site 1 of ^{63}CuHbA and ^{63}CuHbS are very similar to those of the single metal ion environment in CuMb. Site 1 of CuHb is thus

Table III. Comparison of ESR Spectral Parameters in Some Cu(II)–Porphyrin Environments

	$g_\parallel$	$A_\parallel(^{63}Cu)$,[a] cm^{-1}
CuTPP[b] in chloroform (no axial ligand)	2.187	209.0
CuTPP in H_2TPP[c] (no axial ligand)	2.190	210.0
CuTPP–1-methylimidazole (strong axial ligand)[d]	2.225	186.0
CuHb site 1	2.217[e]	179.3[e]
CuHb site 2	2.178[c]	193.6[f]

[a] A values in 10 cm × 10^4. [b] TPP is tetraphenylporphyrin. [c] Reference 26. [d] Reference 25. [e] Consistent with the presence of axial ligands. [f] Consistent with the absence of axial ligands.

presumably five coordinated with one strong axial ligand as has previously been concluded for CuMb.[25] The ligation for site 2 can be inferred by a comparison (Table III) of known ESR spectra parameters of copper tetraphenylporphyrin (TPP) with and without ligation. As seen in Table III, the removal of axial ligands by using $CHCl_3$ as a solvent or using CuTPP doped with H_2TPP[26] results in a decrease of $g_\parallel$ and a concomitant increase in the magnitude of $A_\parallel(^{63}Cu)$.

On the basis of a comparison of the ESR parameters of these model hemes with those of site 2 of ^{63}Cu–hemoglobin, it can be concluded that site 2 has considerably weaker axial ligation than site 1. In fact the parameters for site 2 are similar to, but not identical with, those of TPP without any axial ligands. These results are consistent with the Raman data on NiHbA[27] which suggest a mixture of five-coordinated and four-coordinated Ni–porphyrin complexes.

Additional information as to the nature of bonding in sites 1 and 2 can be obtained from an analysis of the $A(^{63}Cu)$ and $A(^{14}N)$ tensor values. The $A(^{63}Cu)$ tensor has the form

$$|T_{xx}, T_{yy}, T_{zz}| = |A_{xx} - a, A_{yy} - a, A_{zz} - a| \quad (2)$$

where $A_{xx} = A_{yy} = A_\perp$ and $A_{zz} = A_\parallel$ are the observed splittings for an axially symmetric species expected for a porphyrin complex. The isotropic value for the hyperfine splitting, a in eq 2, is equal to $^1/_3(A_\parallel + 2A_\perp)$. For site 1 the anisotropic dipolar contribution to the hyperfine part gives $T_{zz} = -107.93$ G, $T_{xx} = T_{yy} = 53.9$ G, and an isotropic contribution of $a = -65.27$ G. The corresponding values for site 2 are $T_{zz} = -113.95$ G, $T_{xx} = T_{yy} = 56.98$ G, and $a = -76.45$ G, taking the experimental A-tensor values to be negative.[28]

Generally, for a d^9 system, $g_\parallel \gg 2$ combined with the presence of the in-plane nitrogen atoms of the porphyrin moiety favors an electronic configuration in which the unpaired electron is essentially located in the $d_{x^2-y^2}$ orbital. The unpaired spin density in the central metal ion $3d_{x^2-y^2}$ and 4s orbitals of the metal ion can be calculated from the values of the $A(^{63}Cu)$ tensor by using the expressions $T_{zz} = -^4/_7P$ and $T_{xx} = T_{yy} = +^2/_7P$ where $P = g_e g_n \beta_e \beta_n / \langle r^{-3} \rangle d_{x^2-y^2}$ and $a = (8\pi/3) g_n \beta_n g_e \beta_e |\psi_{4s}|^2$.

These calculations further require values for one electron in the $3d_{x^2-y^2}$ and 4s orbitals based on atomic wave functions. We have used the values of Goodman and Raynor[29] for which $-^4/_7P$ is −250 G for one electron in the $3d_{x^2-y^2}$ orbital and a is equal to −1767 G for one electron in the 4s orbital. The calculated spin density values in these metal orbitals for sites 1 and 2 are given in Table IV. This calculation reveals that only half of the total spin is found on the metal with the remaining density delocalized on the porphyrin ring.

It is also possible to determine how the remaining density is delocalized on the porphyrin moiety by the use of molecular orbitals in which the unpaired electron is situated.[30] By the use of C_{4v} or D_{4h} as the ideal symmetry for sites 1 and 2, the principal MO is

$$\psi(b_1, b_{1g}) = \beta_1 d_{x^2-y^2} - \beta_1' {}^1/_2(\sigma_1 - \sigma_2 + \sigma_3 - \sigma_4) \quad (3)$$

where the σ_i are the four hybridized nitrogen orbitals projecting toward the central atom. The normalization condition is

$$\beta_1^2 + \beta_1'2 - 2\beta_1\beta_1' S = 1 \quad (4)$$

where S, the group overlap integral

$$S = 2\langle d_{x^2-y^2} | \sigma_i \rangle \quad (5)$$

has a value of 0.092 for CuTPP.[26] The values of the coefficients β_1 and β_1' are obtained from the observed ^{14}N hyperfine splittings. Such superhyperfine interactions in metalloporphyrins and phthalocyanins have been considered in detail by many authors.[26,31-35]

First we make the dipolar corrections to the observed splitting from ^{14}N nuclei, i.e.,

$$A_\parallel'(^{14}N) = A_\parallel - A_D \qquad A_\perp'(^{14}N) = A_\perp + 2A_D \quad (6)$$

where $A_\parallel'$ and $A_\perp'$ are the values after dipolar corrections and

$$A_D = g_e \beta_e g_n \beta_n / R^3 = 0.2 \times 10^{-4} \text{ cm}^{-1} \quad (7)$$

with the Cu–N bond distance R being taken as 2.0 Å.

These dipolar corrected values may then be used to determine the fractions of 2s and 2pσ contributions to the unpaired spin density on ^{14}N, viz., f_s and f_σ:

$$A_\parallel'(^{14}N) = (8\pi/3) g_e \beta_e g_n \beta_n |\Phi(2s)|^2 f_s^N - {}^2/_5 g_e \beta_e g_n \beta_n \langle r^{-3} \rangle_{2p} f_p^N \sigma \quad (8)$$

$$A_\perp'(^{14}N) = (8\pi/3) g_e \beta_e g_n \beta_n |\phi(2s)|^2 f_s^N + {}^4/_5 g_e \beta_e g_n \beta_n \langle r^{-3} \rangle_{2p} f_p^N \sigma \quad (9)$$

Now the expressions for f_s^N and $f_p^N\sigma$ are

$$f_s^N = \frac{(2A_\parallel' + A_\perp')}{8\pi g_e \beta_e g_n \beta_n |\phi(2s)|^2} \quad (10)$$

and

$$f_p^N \sigma = (({}^1/_3)({}^5/_2)) \frac{A_\perp' - A_\parallel'}{g_e \beta_e g_n \beta_n \langle r^{-3} \rangle_{2p}} \quad (11)$$

By the use of the values[28] of $|\phi(2s)|^2$ and $\langle r^{-3} \rangle_{2p}$ for ^{14}N, viz., 4.814 and 3.0205 au, respectively, the calculated spin densities on the coordinating atoms, namely the pyrrole nitrogens of the heme (sites 1 and 2), are given in Table IV.

Table IV. Experimental Unpaired Spin Densities (in %) in the Various Orbitals[a]

	site 1	site 2
$3d_{x^2-y^2}$ (Cu)	45.32	47.86
4s (Cu)	3.60	4.33
2s (^{14}N)	2.8 (2.86)	2.9
pσ (^{14}N)	0.86 (3.01)	6.02
total (metal)	48.92	52.19
total (pyrrole N)	14.64 (23.48)	35.68
total (metal + N)	63.56 (72.40)	87.87

[a] Values in parentheses for site 1 are based on an error in A of < 1 G and an upper limit of 15.4 × 10^{-4} cm^{-1} for A.

(26) Manoharan, P. T.; Rogers, M. T. In *ESR of Metal Complexes*; Yen, T. F., Ed.; Plenum: New York, 1969; pp 143–173.
(27) Shelnutt, J. R.; Alston, K.; Ho, J.-Y.; Yu, M.-T.; Yamamoto, T.; Rifkind, J. M. *Biochemistry* **1986**, *25*, 620.
(28) McGarvey, B. R. *J. Phys. Chem.* **1967**, *71*, 51.
(29) Goodman, B. A.; Raynor, J. B. *Adv. Inorg. Chem. Radiochem.* **1970**, *13*, 135.
(30) Findlay, M. C.; Dickinson, L. C.; Chien, J. C. W. *J. Am. Chem. Soc.* **1977**, *99*, 5168.
(31) Assour, J. M. *J. Chem. Phys.* **1965**, *43*, 2477.
(32) Deal, R. M.; Ingram, D. J. E.; Stinivasan, R. In *Electron Magnetic Resonance and Solid Dielectrics*; Servant, R., Charnu, A., Eds.; North Holland: Amsterdam, 1964; p 239.
(33) Abkouitz, M.; Chen, I.; Sharp, J. H. *J. Chem. Phys.* **1968**, *48*, 4561.
(34) Kivelson, D.; Neiman, R. *J. Chem. Phys.* **1961**, *35*, 149.
(35) Brown, T. G.; Hoffman, B. M. *Mol. Phys.* **1980**, *39*, 1073.

It is clear from Table IV that even after the inclusion of the pyrrole 2s and 2pσ orbitals a major fraction of the spin density is still not accounted for, particularly for site 1 where only 63.5% (to 72.4%) of the spin density is determined (Table IV). The rest of the unpaired density should be accounted for by σ-delocalization beyond the nitrogen of the pyrrole ring into the carbon σ-framework[36] as well as delocalization originating from π-bonding. This has support from the work of Brown and Hoffman[35] wherein they have observed the spin density on the protons of CuTPP and AgTPP by using ENDOR spectroscopy. Considering the number of possible atoms involved in delocalization of spin density on the porphyrin, one can safely account for the remaining spin density on site 1 and site 2. This conclusion also means that the wave functions of the type

$$\psi = \beta_1\psi_{d_{x^2-y^2}} - \beta_1'{}^1/_2(\sigma_1 - \sigma_2 + \sigma_3 - \sigma_4) \qquad (12)$$

to describe the MO of the unpaired electron are quite inadequate,[35] since the σ_i's in eq 12 represent only the hybrid σ orbitals on the nitrogen of the pyrrole ring, therefore excluding the possible extension to the porphyrin carbon centers.

Another interesting aspect is the nature of the hybridization for the σ-orbital on ^{14}N which is derived from the relative 2s and 2pσ spin densities. The expected hybridization is sp^2 on the basis of a bond angle of 120° at the pyrrole nitrogen. While it is nearly sp^2 for the nitrogens of site 2, the hybridization is less than or equal to sp for those of site 1. It is the value of $A_\perp$ (and hence $A_\perp'$) due to ^{14}N in eq 11 that determines the p character of the orbital spin density. In view of the excellent simulation of the site 1 ESR spectra due to CuMb as well as the excellent combined simulation of sites 1 and 2 in CuHbA, the error in the determination of $A_\perp$ cannot be >1 G, and an upper limit of 15.4×10^{-4} cm^{-1} can be set for $A_\perp$. Therefore, the pσ-spin density is $\lesssim 3.01\%$, and the nitrogen in site 1 is at the maximum sp hybridization (Table IV).

It is well-known[35,37] that a decrease in the expected sp^2 hybridization is indicative of π-bonding, and hence in the case of site 1, the involvement of π-bonding must be greater than in the case of site 2. It has, moreover, been shown[35] in the case of CuTPP and AgTPP that the out-of-plane π-bonding arising from axial ligands is more important than the in-plane π-bonding in porphyrin complexes. Therefore, the axial ligand, i.e., the proximal histidine, perturbs the heme copper in site 1 by both σ- and out-of-plane π-interaction and must be located further from the metal center. π-Delocalization in site 1 also explains the decrease in metal ion spin density (Table IV). Any further attempt to calculate the bonding coefficients from the current data is not justified and must await future ENDOR and ESEEM studies on these reconstituted hemoglobins.

The combination of the visible and ESR spectra for CuHbA and CuMb permits the assignment of the longer wavelength Soret band (seen also in reconstituted myoglobin) to the five-coordinated complex (site 1) and the shorter wavelength Soret band seen only in hemoglobin to much weaker axial ligation (site 2). McLees and Caughey[38] have studied the electronic spectra of divalent nickel(II) porphyrins in the absence and presence of nitrogenous bases. These studies indicate that in noncoordinating solvents such as chloroform, the Soret band lies between 392 and 401 nm depending on the particular solvent. The addition of nitrogenous bases to nickel(II) porphyrin reveals the emergence of a new band at longer wavelength, which is the only band present in solutions of nickel(II) porphyrins in pure nitrogenous bases. The band positions in noncoordinating and coordinating solvents correspond with those of the short wavelength and long wavelength bands found in NiHbA, confirming our interpretation as to the nature of the two species in NiHbA and CuHbA. The recent Raman data on NiHb with 406.7-nm and 413.1-nm excitation furthermore confirm that the longer wavelength Soret band corresponds to a five-coordinated Ni–porphyrin and that the shorter wavelength band shows insignificant axial coordination.[27]

Protein Conformation and the Metal Ion Environment. Although the ESR and visible spectra indicate that both myoglobin and the longer wavelength hemoglobin component are five coordinated, a closer look at the spectral parameters for both of these species indicates small differences. The Soret bands for CuMb and NiMb are thus shifted 6–7 nm further to the red. This observation is consistent with Raman data[27] on the Ni(II)-substituted proteins which suggest a stronger proximal histidine bond in myoglobin than in hemoglobin. The decrease in $g_\parallel$ of 0.003 for myoglobin relative to hemoglobin is probably not significant, although the 0.009 decrease in $g_\perp$ is probably significant as indicated by the almost identical values of $g_\perp$ for HbA and HbS and would suggest a decrease in the axial ligand π-bonding for myoglobin.

These differences between the Ni- and Cu-substituted myoglobin and the five-coordinated hemoglobin species can be attributed to differences between the T-quarternary structure found to be present in Ni(II)- and Cu(II)-substituted hemoglobin[19,24] and the tertiary structure more analagous to the R conformation in myoglobin.

The comparison between metal-substituted myoglobins with an R-type conformation and metal-substituted hemoglobins with a T-type conformation would also seem to suggest that the R-type conformation produces the five-coordinated heme environment, while the T-type conformation results in constraints which produce a mixture of two metal ion environments in a single electrophoretically pure protein. However, the visible spectra of the α-sH subunits and the β-SH tetramer (Table I, Figure 2) indicate a more complex picture.

The short wavelength band in the R-type monomeric α-SH subunit and the long wavelength band in R-type myoglobin indicate that the particular metal ion coordination is not determined by the T- or R-like structure, but some other aspect of the local heme environment. It is difficult at this point to delineate the specific factor(s) responsible for this change in the metal ion coordination. It may, however, be related to the finding that the distal side of the heme pocket is much more flexible in the R-state α-chain than in myoglobin.[39,40]

The enhanced flexibility in hemoglobin has been shown to produce interactions between the metal ion and the distal histidine[41] which are not detected in myoglobin.[42] The favored site 2 coordination with much weaker axial ligation in the hemoglobin isolated α-chains as opposed to myoglobin may thus reflect a weakening of the proximal histidine bond resulting from weak distal histidine interactions.

Ni^{II}-β-SH consists of a β_4 tetramer.[43] Although the high affinity for 2,3-diphosphoglyceric acid[43] and the unit cell dimensions of the β_4 crystal[44] suggest a possible T-like structure, this tetramer which binds oxygen noncooperatively with a high affinity[43] is considered to be in an R-like conformation.[45] The presence of split Soret for Ni^{II}-β-SH and NiHbA therefore suggests that the presence of two metal ion environments is not directly related to the quaternary T or R conformation, but it does require a tetramer where subunit interactions produce constraints which influence metal ion coordination.

In conclusion, our results seem to require three levels at which the metal ion coordination in Ni(II)- and Cu(II)-substituted hemeproteins are influenced by protein conformation. (1) In monomeric proteins the type of coordination is determined by the protein conformation in the heme pocket. (2) In tetrameric proteins, subunit interactions can produce a mixture of two types

(36) LaMar, G. N. In *NMR of Paramagnetic Molecules*; LaMar, G. N., Horrocks, W. Dew., Holm, R. H., Eds.; Academic: New York, 1973; pp 86–128.
(37) Manoharan, P. T.; Subramanian, S., unpublished results.
(38) McLees, B. D.; Caughey, W. S. *Biochemistry* **1968**, *7*, 642.
(39) Shaanan, B. *J. Mol. Biol.* **1983**, *171*, 31.
(40) Case, D. A. In *Hemoglobin and Oxygen Binding*; Ho, C., Ed.; Elsevier Biomedical: New York, 1982; pp 371–375.
(41) Levy, A.; Rifkind, J. M. *Biochemistry* **1985**, *24*, 6050.
(42) Levy, A.; Alston, K.; Rifkind, J. M. *J. Biomol. Struct. Dynam.* **1984**, *1*, 1299.
(43) Benesch, R.; Benesch, R. E.; Enoki, Y. *Proc. Natl. Acad. Sci. U.S.A.* **1968**, *61*, 1102.
(44) Perutz, M. F.; Mazzarella, L. *Nature (London)* **1963**, *199*, 639.
(45) Arnone, A.; Briley, P. D.; Rogers, P. H.; Hendrickson, W. A. In *Hemoglobin and Oxygen Binding*; Ho, C., Ed.; Elsevier Biomedical: New York, 1982; pp 127–133.

of coordination in individual proteins. (3) Effects on the proximal histidine associated with the R ⇄ T quaternary conformation influence the five-coordinated sites.

Acknowledgment. We express our sincere thanks to Prof. James Hyde and Dr. William Antholine for allowing us to perform the Q-band ESR measurements at the National Biomedical ESR Center at Milwaukee, WI. We also thank Dr. Periannan Kuppusamy for valuable suggestions.

Registry No. NiHbA, 82029-96-7; CuHbA, 82029-94-5; CuHbS, 82030-03-3; Ni, 7440-02-0; Cu, 7440-50-8; L-histidine, 71-00-1.

Communications to the Editor

Synthesis of (±)-Fredericamycin A

T. Ross Kelly,* Naohito Ohashi,
Rosemary J. Armstrong-Chong, and Stephen H. Bell

Department of Chemistry, Boston College
Chestnut Hill, Massachusetts 02167

Received May 13, 1986

The 1982 report[1] of the unusual structure **1** and exceptional anticancer activity of fredericamycin A has generated considerable attention.[2,3] We now report the synthesis of (±)-fredericamycin A.

The synthetic strategy was to first construct synthons for the top and bottom units of **1** and to then effect their coupling in conjunction with elaboration of the spiro center, a process which was envisaged to commence with acylation of **2a** by **4**. Synthesis of **2a** was achieved (Scheme I) by three consecutive metalation reactions which serve to annelate the pyridone ring onto the methoxymethyl ether (**5**) of commercially available 4-indanol. Anhydride **4** was secured by the route outlined in Scheme II. Both **2a** and **4** are routinely prepared in 5–10-g batches.

It had been our hope that the MOM group in **2a** might facilitate

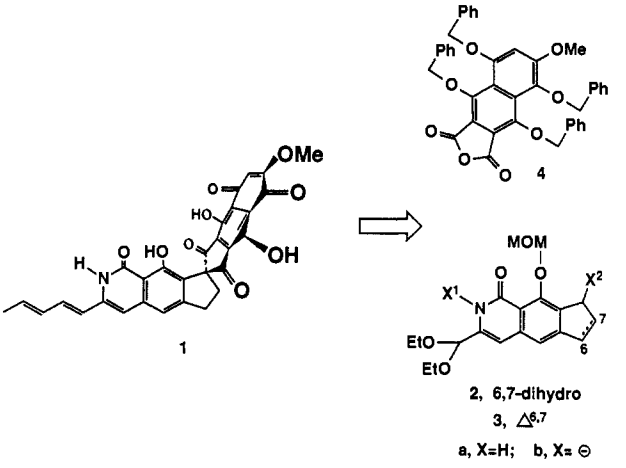

lateral[13] metalation of the adjacent benzylic carbon to give **2b**, thereby setting the stage for condensation with **4**. Unfortunately, lateral metalation of **2a** could not be achieved. Replacement of the MOM group with other possible activating groups (e.g., MEM,[14] $CH_2CH_2NMe_2$,[15] and OC(=O)NHMe[16]) was also unavailing. Attempts to carry the benzylic anion forward in a latent form (**2a**, X^2 = Br or $SnMe_3$) foundered due to the instability of intermediates.

In contrast to indane **2a**, indene **3a** [also regularly prepared (Scheme I) on a 5–10-g scale] could be converted in high yield to the corresponding anion **3b** under carefully defined conditions (3.2 equiv of *t*-BuLi, THF, −78 °C, 30 min) and **3b** is smoothly acylated by **4**. But while use of **3a** in place of **2a** solves the metalation problem, a new complication is introduced: the allylic

(1) (a) Misra, R.; Pandey, R. C.; Silverton, J. V. *J. Am. Chem. Soc.* **1982**, *104*, 4478–4479. For related papers, see: (b) Pandey, R. C.; Toussaint, M. W.; Stroshane, R. M.; Kalita, C. C.; Aszalos, A. A.; Garretson, A. L.; Wei, T. T.; Byrne, K. M.; Geoghegan, R. F., Jr.; White, R. J. *J. Antibiot.* **1981**, *34*, 1389–1401. (c) Warnick-Pickle, D. J.; Byrne, K. M.; Pandey, R. C.; White, R. J. *Ibid.* **1981**, *23*, 1402–1407. (d) Byrne, K. M.; Hilton, B. D.; White, R. J.; Misra, R.; Pandey, R. C. *Biochemistry* **1985**, *24*, 478–486.

(2) *Chem. Eng. News.* **1982**, Aug 16, p 27; **1983**, Sept 19, pp 36–37.

(3) For reports of model studies on the construction of the spiro system of **1**, see: (a) Rama Rao, A. V.; Reddy, D. R.; Deshpande, V. H. *J. Chem. Soc., Chem. Commun.* **1984**, 1119–1120. (b) Parker, K. A.; Koziski, K. A., Breault, G. *Tetrahedron Lett.* **1985**, *26*, 2181–2182. (c) Kende, A. S.; Ebetino, F. H.; Ohta, T. *Ibid.* **1985**, *26*, 3063–3066. (d) Eck, G.; Julia, M.; Pfeiffer, B.; Rolando, C. *Tetrahedron Lett.* **1985**, *26*, 4723–4724. (e) Eck, G.; Julia, M.; Pfeiffer, B.; Rolando, C. *Ibid.* **1985**, *26*, 4725–4726. (f) Braun, M.; Veith, R. *Ibid.* **1986**, *27*, 179–182. (g) Bach, R. D.; Klix, R. C. *J. Org. Chem.* **1986**, *51*, 749–752. (h) Bennett, S. M.; Clive, D. L. J. *J. Chem. Soc., Chem. Commun.* **1986**, 878–888. For another approach to a bottom-half synthon for **1** see: Parker, K. A.; Breault, G. A. *Tetrahedron Lett.* **1986**, *27*, 3835–3838.

(4) (a) For a leading reference, see: Sibi, M. P.; Snieckus, V. *J. Org. Chem.* **1983**, *48*, 1935–1937. (b) See also: Gschwend, H. W.; Rodriguez, H. R. *Org. React.* **1979**, *26*, 1–360.

(5) Beak, P.; Snieckus, V. *Acc. Chem. Res.* **1982**, *15*, 306–312.

(6) Compare: Poindexter, G. S. *J. Org. Chem.* **1982**, *47*, 3787–3788. Diethoxyacetonitrile was obtained from Chemical Dynamics Corp.

(7) Prepared (96% overall) in three steps (NaH, CH_3OCH_2Cl, THF; $LiAlH_4$, THF; *t*-$BuSiMe_2Cl$, imidazole, DMF), from 4-hydroxyindan-1-one which is available (88%) by a modification of the known[8] $AlCl_3$-catalyzed isomerization of dihydrocoumarin.

(8) Loudon, J. D.; Razdan, R. K. *J. Chem. Soc.* **1954**, 4299–4303.

(9) Grieco, P. A.; Gilman, S.; Nishizawa, M. *J. Org. Chem.* **1976**, *41*, 1485–1486.

(10) Ansell, M. F.; Nash, B. W.; Wilson, D. A. *J. Chem. Soc.* **1963**, 3028–3036.

(11) For a recent report of a similarly conceived synthesis of **7**, see: Keith, D. D. *Tetrahedron Lett.* **1985**, *26*, 5907–5910. See also: Thiele, J.; Gunther, F. *Ann.* **1906**, *349*, 45–60.

(12) Compare Homeyer, A. H.; Wallingford, V. H. *J. Am. Chem. Soc.* **1942**, *64*, 798–801.

(13) See, inter alia: (a) Gilman, H.; Morton, J. W., Jr. *Org. React.* **1954**, *8*, 258–304 (see especially pp 260 and 278). (b) Wakefield, B. J. *The Chemistry of Organolithium Compounds*; Pergamon Press: Oxford, England, 1974; p 30. (c) Vaulx, R. L.; Puterbaugh, W. H.; Hauser, C. R. *J. Org. Chem.* **1964**, *29*, 3514–3517. (d) Harmon, T. E.; Shirley, D. A. *Ibid.* **1974**, *39*, 3164–3165. (e) Ludt, R. E.; Crowther, G. P.; Hauser, C. R. *Ibid.* **1970**, *35*, 1288–1296. (f) Vaulx, R. L.; Jones, F. N.; Hauser, C. R. *Ibid.* **1964**, *29*, 1387–1391. (g) Cabiddu, S.; Melis, S.; Piras, P. P.; Sotgiu, F. *J. Organometal. Chem.* **1979**, *178*, 291–300. (h) Beak, P.; Tse, A.; Hawkins, J.; Chen, C.-W.; Mills, S. *Tetrahedron* **1983**, *39*, 1983–1989. (i) Footnote 8 in: Watanabe, M.; Sahara, M.; Furukawa, S.; Billedeau, R.; Snieckus, V. *Tetrahedron Lett.* **1982**, *23*, 1647–1650. (j) References 4b and 5.

(14) Ellison, R. A.; Kotsonis, F. N. *J. Org. Chem.* **1973**, *38*, 4192–4196.

(15) Amupitan, J.; Sutherland, J. K. *J. Chem. Soc., Chem. Commun.* **1978**, 852–853. Köster, F.-H.; Wolf, H. *Tetrahedron Lett.* **1981**, *22*, 3937–3940.

(16) Compare ref 4a.

(17) Hopkins, G. C.; Jonak, J. P.; Minnemeyer, H. J.; Tieckelmann, H. *J. Org. Chem.* **1967**, *32*, 4040–4044.

(18) (a) For reviews of the synthesis of spiro compounds, see: Krapcho, A. P. *Synthesis* **1974**, 383–419; **1976**, 425–444; **1978**, 77–126. (b) A similar reduction/aldol sequence has been reported: Holland, H. L.; MacLean, D. B.; Rodrigo, R. G. A.; Manske, R. F. H. *Tetrahedron Lett.* **1975**, 4323–4326. We thank Prof. Rodrigo for bringing the similarity of this reaction to our attention. (c) To date putative one-step conversions of **17** to **19** (e.g., with methoxide) have failed.

(19) Herscovici, J.; Antonakis, K. *J. Chem. Soc., Chem. Commun.* **1980**, 561–562.

(20) Bohlmann, F.; Mannhardt, H.-J. *Chem. Ber.* **1956**, *89*, 1307–1315.

0002-7863/86/1508-7100$01.50/0